

Guided Interpretable Facial Expression Recognition via Spatial Action Unit Cues

Soufiane Belharbi¹, Marco Pedersoli¹, Alessandro Lameiras Koerich¹, Simon Bacon², and Eric Granger¹

¹ LIVIA, Dept. of Systems Engineering, ÉTS, Montreal, Canada

² Dept. of Health, Kinesiology & Applied Physiology, Concordia University, Montreal, Canada

soufiane.belharbi@etsmtl.ca

ABSTRACT

While state-of-the-art facial expression recognition (FER) classifiers achieve a high level of accuracy, they lack interpretability, an important aspect for end-users. To recognize basic facial expressions, experts resort to a codebook associating a set of spatial action units to a facial expression. In this paper, we follow the same expert footsteps, and propose a learning strategy that allows us to explicitly incorporate spatial action units (AUs) cues into the classifier’s training to build a deep interpretable model. In particular, using this AUs codebook, input image expression label, and facial landmarks, a single action units heatmap is built to indicate the most discriminative regions of interest in the image w.r.t the facial expression. We leverage this valuable spatial cue to train a deep interpretable classifier for FER. This is achieved by constraining the spatial layer features of a classifier to be correlated with AUs map. Using a composite loss, the classifier is trained to correctly classify an image while yielding interpretable visual layer-wise attention correlated with AUs maps, simulating the experts’ decision process. This is achieved using only the image class expression as supervision and without any extra manual annotations. Moreover, our method is generic. It can be applied to any CNN- or transformer-based deep classifier without the need for architectural change or adding significant training time. Our extensive evaluation¹ on two public benchmarks RAF-DB, and AffectNet datasets shows that our proposed strategy can improve layer-wise interpretability without degrading classification performance. In addition, we explore a common type of interpretable classifiers that rely on Class-Activation Mapping methods (CAMs), and we show that our training technique improves the CAM interpretability.

Keywords: Facial Expression Recognition, Interpretability, Action Units, Deep Models, Weakly-supervised Object Localization, Class Activation Maps (CAMs).

1 Introduction

Facial expression recognition (FER) has recently received much interest in the computer vision and machine learning communities [8, 82, 92]. Since facial expression is one of the

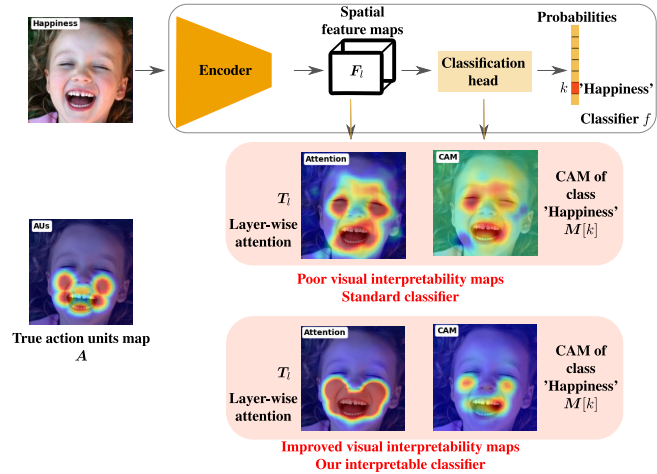


Figure 1: Comparison between standard non-interpretable and our interpretable FER classifier at inference time. Our classifier yields attention and CAM that are aligned with the expert’s knowledge used to assess basic facial expressions in images [51], which is illustrated in the map A . Consequently, our model’s decision is more reliable. This is achieved without compromising the classification accuracy of our model. Details of our training strategy is presented in Fig.3. Note that in CAM-based models the classification head can be a fully convolutional module or standard fully connected layers that pooled posterior probabilities.

most important ways for people to express emotions [16], FER finds a wide range of applications in, e.g., medical analysis and monitoring [1, 35, 84], eHealth [68], driver fatigue detection [2, 46], safe driving [33], security [41, 58], lecturing [69], and many other fields [63].

FER remains challenging, particularly for in real world applications. This is due to the subtle differences between expressions, leading to low inter-class variability. As a result, learning to separate classes becomes difficult. This sets apart the FER task from standard classification problems, where classes are typically easy to distinguish. Additionally, people express the same facial expression differently depending on variant attributes such as level of expressiveness, age, gender, and ethnic background [38, 71]. To tackle these challenges, many deep methods have been proposed to build highly accurate models [8, 38, 82, 92]. This is achieved

¹Code: <https://github.com/sbelharbi/interpretable-fer-aus>.

by learning deep, robust feature representations compared to traditional hand-crafted features [15, 47, 67]. Deep FER methods usually rely on either global or local approaches to learn feature representations. Global approaches [24, 39] propose training losses to improve representation robustness. To avoid incorporating noise into the global image representation, local approaches resort to learning from parts of the image [8, 30, 40, 74, 79, 80, 82, 92]. These methods use facial landmarks to extract robust features around relevant parts of the face [30, 79, 92]. Other methods rely on self-attention mechanisms to focus on relevant and discriminative parts of the image and suppress noisy regions [8, 40, 74, 80, 82].

State-of-the-art FER methods for classification have achieved great progress in term of accuracy. However, in multiple critical applications such as eHealth [17, 61, 94], end-users may not require only an accurate classifier that yields a classification score. They may be also interested in an interpretable decision of the model [17, 83, 94]. For instance, this can help clinicians and therapists understand and build trust in the FER model’s decisions, planning better subsequent future interventions [72]. Subsequently, this facilitates better integrating machine learning-based models into daily clinical routines and health care practice [72]. In addition, interpretability can greatly help diagnose errors made by machine learning models and facilitate the identification of weaknesses for future improvement. Unfortunately, interpretability has been overlooked and shadowed in the FER task due to the main focus on classification accuracy. This has led to the design of FER models that lack interpretability. Recent attention-based works such as APVIT [82] build explicitly internal attention to select only discriminative regions of interest (ROIs). Although they provide visual interpretability to highlight the used regions for the classification, such ROIs are not necessarily aligned with what experts typically use to assess facial expressions. Commonly, experts rely on a codebook of action units to determine a basic facial expression [51] (Fig. 2). Each basic facial expression is associated with a subset of spatial action units in the face. Ideally, an interpretable classifier should point to and localize the correct action units’ ROIs when predicting a facial expression. However, this is a challenging task since predicting such ROIs using only image expression supervision is not trivial. Additionally, these localization cues are not publicly available to be learned since they burden the annotation cost and complicate building large-scale benchmarks.

This work proposes a generic learning strategy to build an interpretable deep classifier for the FER task. This is achieved using spatial action units cues constructed from the image class supervision without extra manual annotation cost. This explicitly integrates the expert approach for facial expression assessment into the decision-making of a classifier. In particular, we build a visual interpretability tool consistent with action units cues used by experts [51]. To this end, we con-

struct a spatial discriminative heatmap that gathers relevant locations of action units required to determine the expression in an input image. Then, layer-wise deep features of a classifier are constrained to be correlated with such heatmap cues during training. At the same time, the model is trained to correctly classify the image. Such a multi-task training scheme allows to build accurate but, most importantly, interpretable classifiers. During inference, the layer-wise attention plays the role of a visual interpretability tool that indicates which ROIs are used to determine the predicted expression (Fig. 3, 1). This is achieved without any extra manual annotation cost, as illustrated in Fig. 3. Discriminative action units heatmap can be built simply using image class expression, action units codebook, and facial landmarks, commonly estimated using off-the-shelf methods. Note that typically, interpretability in models usually emerges as a result of other tasks, such as classification without explicit supervision for interpretability [19]. It comes as a tool to clarify the model decision, for instance, under the form of visual ROIs. However, since we explicitly provide interpretability cues to train our model, we refer to it as *guided* interpretable FER model.

Following the interpretable classifier direction, we explore a curated branch of classifiers in this work that allows us to perform image classification and yield visual interpretability. In particular, we visit Class-activation maps (CAMs)-based classifiers [12, 62]. Such models are popular in the weakly-supervised object localization task (WSOL) in computer vision for different imaging types, including natural scene [93] and medical imaging [62, 73]. Given an input image, such classifiers can be trained using only image class labels to correctly classify an image and provide a per-class heatmap, i.e., CAM, to localize ROIs related to the image class. Therefore, they play an important role in localization and interpretability, making them well-suited for our focus in this work. Therefore, we conduct a comparative study of different CAM-based methods from different families and assess their classification and interpretability capacity for the FER task. We note that this is the first work to leverage CAM-based methods for the FER task.

Our main contributions are summarized as follows:

- (1) Unlike standard non-interpretable FER classifiers, we propose a generic learning strategy to build an accurate but, most importantly, interpretable deep classifier (Fig.1). The interpretability is consistent and aligned with the process used by experts to determine basic facial expressions, which relies on spatial action units.
- (2) Our method does *not*: add any extra manual annotation, add significant extra computations during training, or change the model architecture or the inference process. In addition, our method is generic. It can be used with any deep CNN or transformer-based model.

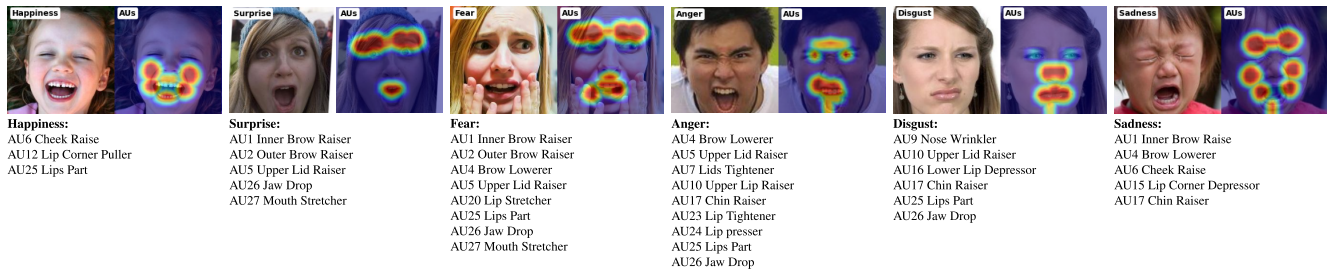


Figure 2: Codebook of basic facial expressions and their associated action units [51]. The spatial action units map is built using the image expression to select the right corresponding action unit subset in combination with facial landmarks which are employed to localize these same action units in the image properly. The code 'AUx' is the identifier of the action unit [51].

(3) Our approach is validated over two public FER benchmarks: RAF-DB, and AffectNet by quantifying both classification and interpretability accuracy. We evaluated different CAM-based methods with and without our spatial action units cues. Different ablations are provided as well.

(4) Empirical results showed that both classification and interpretability improve with our method. Interestingly, compared to a vanilla deep classifier, we show that its layer-wise attention can largely be shifted using our action units' spatial cues without compromising classification accuracy. In fact, we show that classification accuracy improves, particularly over large datasets such as AffectNet. This demonstrates that, indeed, spatial action units are a reliable source for discriminative ROIs for basic facial expression recognition [51].

2 Related Work

This review covers related work on FER classifier systems, CAM-based methods for localization and interpretability, interpretability in FER systems, and finally, action units in FER task.

Standard FER classification methods. With the availability of large public benchmarks [39, 53], different methods have been proposed aiming to achieve state-of-the-art classification accuracy [38]. This is most achieved by designing robust features to overcome the limitations of traditional hand-crafted features [15, 47, 67]. Building robust features is tackled by deep models either via a global or local approach.

Global methods typically focus on designing robust training losses to build enhanced discriminative features while using the entire image to build a global representation [24, 39]. For instance, Farzaneh and Qi [24] leverage deep metric learning and propose a deep attentive center loss to select a subset of relevant features for classification adaptively. Although successful, image faces are typically noisy, which may easily corrupt the features. Local methods tackle this issue by explicitly incorporating different mechanisms to remove the noise and build better features. Mainly, these meth-

ods rely on a part-based approach assuming that only some regions in the image are relevant to determine the expression [8, 30, 40, 74, 79, 80, 81, 82, 92].

A subset of these methods assumes that discriminative features are located around facial landmarks. Therefore, only these regions are cropped either at image or spatial feature level [30, 79, 92]. This assumes that relevant regions are located around the landmarks. Such early dropout of patches may discard relevant patches not included in the landmarks in addition to missing the context. This also requires highly accurate landmarks. However, leveraging landmarks has been successful in the recent work POSTER [50, 92] by cross-fusion of sparse key-landmarks features with standard global image features.

A second subset exploits attention mechanism [8, 80, 74, 81, 82] either self-learned or with provided cue. DAM-CNN [80] learns a spatial feature attention to filter out noise and keep only relevant spatial features to build a dense embedding later. The APVIT method [81, 82] leverages transformers and their attention potential to design an FER classifier. In particular, they propose a self-attention approach early in the network. Such attention allows the selection of relevant patch regions and performs hard attention at the spatial feature level. Patches are scored, and only the top-k are allowed to proceed into the next layer to build an image embedding. This explicitly allows the model to learn to filter out irrelevant patches. Other methods are provided external spatial cues to be aware *where* to look for discriminative regions [8, 40, 74]. RAN [74] is a region-based method. It performs image cropping either randomly or using landmarks. Their features are then attended using self-attention and relation-attention modules. Such attention is then used to combine different features and build an image embedding. This makes the final representation robust to pose and occlusion. Li et al. [40] follow a similar direction by decomposing the spatial features into the regions and using the attention module afterward. Bonnard et al. [8] use facial landmarks to build a heatmap, which is used to align spatial features in a deep model. This is expected to filter

out irrelevant spatial features and focus mostly on features around landmarks. Our work is more aligned with this family of methods. However, we use grounded and more reliable cues, that is, spatial action units. Since spatial action units are class-dependent, they are more discriminative for the FER task [51], compared to facial landmarks, which are generic and class-agnostic.

While the aforementioned methods focus on FER over still images, other methods tackle video applications [42, 43, 44, 45]. These methods deal with similar issues presented in still images while leveraging temporal dependency and multi-modality in videos to capture better expressiveness and build robust features.

CAM-based methods for weakly-supervised object localization and interpretability. Using only image class as supervision, CAM-based methods can be trained to classify an image correctly and yield reliable localization of ROIs related to the image class. They are currently the dominant approach for the WSOL task [12, 62]. They achieved interesting results in different domains, including natural scene images [7, 62, 77], and medical imaging [5, 6, 62, 73]. They have been extended to localization in videos as well [3, 4]. Early works have focused on building different spatial pooling layers [20, 21, 59, 93]. However, CAMs tend to highlight only small and most discriminative parts of an object [12, 62], limiting its localization performance. To overcome this, different strategies have been proposed, including data augmentation on input image or deep features [6, 13, 49], as well as architectural changes [29, 36, 77, 90]. Recently, learning via pseudo-labels has shown great potential, despite its reliance on noisy labels [7, 5, 52, 56, 54, 55, 75]. Most previous methods used only forward information in a CNN (bottom-up family [62]). However, other methods aim to leverage backward information as well (top-down methods [62]). These include biologically inspired methods [9, 87], and gradient [10, 28, 34, 66] or confidence score aggregation methods [18, 57]. CAM-based methods have been used for interpretability as well [64, 78] since they provide a map that indicates ROIs relevant to the model’s decision. Gradient-based CAMs are most common in interpretability task [10, 28, 34, 66] in addition to [9, 87]. They mainly search for ROIs in the *feature maps* that better stimulate a class response. This inspires other methods [88] to leverage gradient and extend it to input image and perform perturbation analysis [14, 25, 26, 60, 86] where the aim is to find which ROI of the network’s input that better stimulates its output. Compared to CAM-based, these methods are often expensive in term of computation and require performing an optimization, making them less attractive for FER tasks. However, CAM-based methods are simple to use, and they are built into the model, requiring a single forward or a forward and backward computation.

Interpretability in FER systems. In critical FER applications such as eHealth and behavioral health interventions and assessments [11], it may not enough to simply accurately predict the facial expression. Users may require interpretability to help understand the model decision [17, 61, 83, 94]. Although important, interpretability in FER systems has been largely overlooked. This is mainly due to the sole focus on achieving state-of-the-art classification accuracy over challenging benchmarks [38]. The absence of public datasets with interpretability annotation has also contributed to shadowing such an important task. Some of the recent works have attempted to provide built-in discriminative attention under the form of visual interpretability, such as the APVIT method [81, 82]. These methods are still limited and, most importantly, unreliable since their interpretability has not been quantified yet due to the lack of annotation. In this work, we propose a protocol to evaluate the interpretability of an FER system without the need for extra manual annotation. We resort to using spatial facial action units to simulate experts’ processes to assess expressions [51]. Such action units are built and encoded automatically in a convenient spatial heatmap using only image expression as supervision. This can help to automatically label large benchmarks easily, allowing training and evaluation of FER models in term of interpretability.

Action units in FER systems. The Facial Action Coding System (FACS) is a taxonomy for fine-grained facial expression analysis [22, 27]. They have long been used to analyze facial expressions [23, 32, 48, 65, 91]. Each basic facial expression is associated with a list of action units as they determine which facial muscles are involved in expressing such emotion. The common established task in the literature is action units detection [32, 48]. It is a supervised multi-label classification task. It aims at predicting the correct set of *active* action units in an input image. To perform such a task, a tedious annotation is required to determine the *active* set of action units in each image since not all action units must be active at once. Another related task goes further to estimate the *intensity* of the action units [23, 91] which is furthermore challenging. Other works aim to jointly localize and estimate the intensity [65]. The work of [32] is relatively close to our work. In order to accurately detect active action units through multi-label classification, authors leverage multi-task learning to jointly predict a localization heatmap for the same action units. The goal is to improve action units detection via their spatial localization. However, action units have not been used for the interpretability of FER classifiers. This makes our work the first to do so. To avoid the extra annotation cost burden, we use generic discriminative action units codebook defined in [51]. It allows the automatic labeling of large benchmarks without manual intervention (Fig. 3). The codebook associates a set of action units to a basic facial expression (Fig. 2). This is used to build a discriminative heatmap that holds potential ROIs to be inspected by the model in order to determine the facial

expression in the input image. This does not require all the action units to be active. But, it is more likely that part of them are active in order for the expression to be manifested in an image. A further step of our work is to use active action units to build an ideal interpretable model but it comes at an additional expensive annotation cost. Alternatively, a pretrained action units detector could be used such as [32].

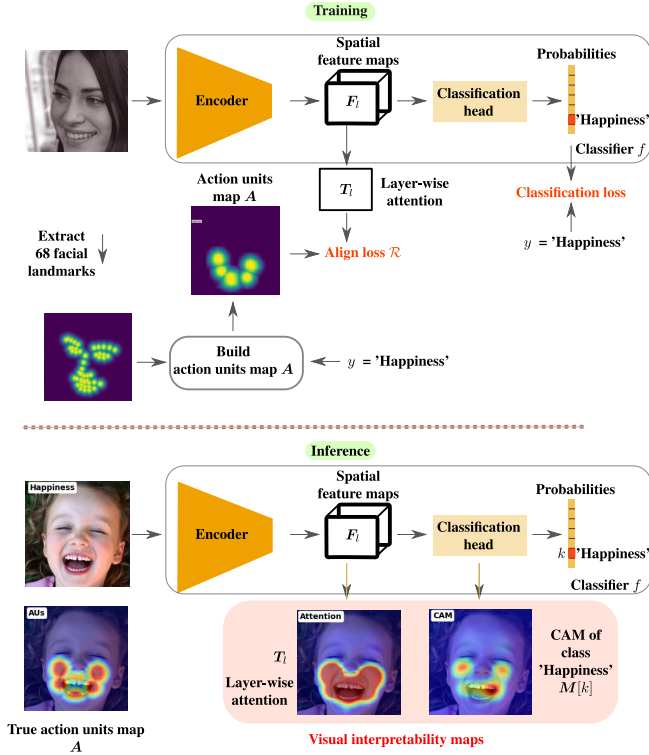


Figure 3: Our interpretable classifier for the FER task (training and inference). Each basic facial expression can be determined via a set of action units [51]. Therefore, to train our interpretable classifier, we first extract facial landmarks and build a *discriminative* spatial map \mathbf{A} that contains the set of all action units associated with the image class expression [51]. This map is used as localization cues to train layer-wise attention T_l to focus on the ROIs highlighted in the action units map. Classification loss, such as cross-entropy, is also used. Once trained, the classifier yields an interpretable layer-wise attention map. When CAM-based classifier [62] is considered, the model can also produce a per-class interpretable map (i.e., CAM).

3 Proposed Approach

3.1 Notation

We denote by $\mathbb{D} = \{(\mathbf{X}, y)_i\}_{i=1}^N$ a training set of N images, where \mathbf{X}_i , of size $h \times w$, is the input image, and

$y_i \in \{1, \dots, K\}$ is its image class, i.e. facial expression, with K is the total number of classes. We denote by $f(\mathbf{X}; \theta)$ a deep classifier with θ its parameters. The posterior per-class probabilities are referred to as $f(\mathbf{X}) \in [0, 1]^K$ where $f(\mathbf{X})_k$ is the probability of the class k . The spatial feature maps produced by the classifier’s encoder at a layer l are a tensor denoted by $F_l \in \mathbb{R}^{n \times h' \times w'}$, where n is the number of feature maps, and $h' \times w'$ is their size which is typically smaller than the input image. CAM-based WSOL methods produce an additional spatial tensor that holds all the CAMs, $M \in \mathbb{R}^{K \times h'' \times w''}$, where $M[k]$ is the CAM of the class k .

3.2 Building spatial action units maps

Given an input image and its label (\mathbf{X}, y) , standard 68 facial landmarks are extracted from the image using off-the-shelf techniques such as SynergyNet [76]. This allows us to *localize* relevant parts of the face such as mouth, nose, eyes, and eyebrows, which will be helpful later to estimate the location of relevant action units. Martinez et al. [51] suggest that each facial expression can be recognized by inspecting a combination of action units (Fig. 2). For instance, the expression ‘Happiness’ involves a set of action units: ‘cheek raise’, ‘lip corner puller’, ‘lips part’. Using the extracted facial landmarks around the mouth part, we can localize the ‘lip part’ of the face. Such localization is translated into a 2D heatmap where strong activations are concentrated around the ‘lip’ to indicate an ROI, and tiny activation everywhere else to indicate background. Such a 2D map is of great importance in training since it provides useful localization cues for relevant discriminative parts in an input image for the FER task used by experts. Typically, this requires manual annotation to delineate ROIs, increasing the annotation cost. Unfortunately, such valuable annotation is not available in public facial expression benchmarks. This work simulates such ROIs *without* an additional manual supervision cost. Using the codebook of facial expressions and their associated action units provided in [51] (Fig. 2), in combination with the extracted facial landmarks and the image label expression y , a single 2D heatmap, $\mathbf{A} \in \mathbb{R}^{h \times w}$, is built to hold all the relevant (i.e., discriminative) action units for the input image (Fig. 3). Consequently, the input image is augmented with an extra supervision cue to be $(\mathbf{X}, y, \mathbf{A})$ where \mathbf{A} is the estimated action units map. To ease subsequent alignment computations, this map is normalized to have values between 0 and 1: $\mathbf{A} \in [0, 1]^{h \times w}$. Note that this process requires only the image class, i.e. image facial expression, as supervision. No extra manual annotations are required.

3.3 Layer-wise attention

Given a layer-wise spatial feature tensor F_l at layer l , we aim to determine which spatial parts are relevant for classification.

A common approach to achieve this is through features self-attention [13, 96]. Such spatial attention is estimated via the average feature map as follows,

$$\mathbf{T}_l = \frac{1}{n} \sum_{j=0}^n \mathbf{F}_l[j], \quad (1)$$

where n is the total number of feature maps. The discrepancy in activations in \mathbf{T}_l differentiates relevant from irrelevant regions. High activations indicate potential spatial ROIs for classification, while low activations point to background and noisy regions. In a deep classifier, such attention maps are a great candidate to incorporate spatial learning cues into the model. We note that although CAM tensors \mathbf{M} hold spatial discriminative cues, they are very sensitive to being altered. Aligning them explicitly with other maps can easily lead to poor classification [7, 12]. Therefore, we rely on layer-wise attention to learn better and interpretable spatial features in this work.

3.4 Action units alignment loss

After estimating both layer-wise attention \mathbf{T}_l and action units map \mathbf{A} , we can proceed with their alignment to train the classifier to yield similar spatial cues. Since the dynamic range of the attention map is unknown beforehand, and since it changes during training, it is inadequate to train the attention to have the same values as the action unit map \mathbf{A} . Instead, we resort to a loss that aims to yield attention maps that are *correlated* with \mathbf{A} . To this end, we use cosine similarity as,

$$\mathcal{R}(\mathbf{T}_l, \mathbf{A}) = \frac{\sum (\mathbf{T}_l \odot \mathbf{A})}{\|\mathbf{T}_l\|_2 \|\mathbf{A}\|_2}, \quad (2)$$

where $\cdot \odot \cdot$ is the Hadamard product, and $\|\cdot\|_2$ is the ℓ^2 norm. Maximizing Eq. 2 pushes the layer l to learn spatial features in a way their mean is highly correlated with the action units map cue \mathbf{A} . In practice, the map \mathbf{A} is downsampled to the same size as \mathbf{T}_l before applying the alignment in Eq. 2.

3.5 Total training loss

Given the triplet $(\mathbf{X}, y, \mathbf{A})$, our goal is to train the classifier f to correctly classify the input image \mathbf{X} to yield the right class y . Additionally, we aim to push the layer l to construct spatial features that are correlated with the action units map cues \mathbf{A} . To achieve this, we jointly minimize the following composite loss,

$$\min_{\theta} -\log(f(\mathbf{X}; \theta)_y) + \lambda(1 - \mathcal{R}(\mathbf{T}_l, \mathbf{A})), \quad (3)$$

where $\lambda \geq 0$ is a weighting coefficient that balances the importance of attention alignment with the action units map compared to cross-entropy loss (left side term). The generalization of Eq. 3 to a combination of multiple layers is straightforward. It can be achieved by adding more layer-wise

terms to the loss. Minimizing Eq. 3 incorporates explicitly the experts' procedure in assessing basic facial expressions in images into the model decision process. The classifier is trained to localize the relevant action units in order to build discriminative features for expression prediction. This justifies using layer-wise attention \mathbf{T}_l as an interpretability tool during inference time (Fig. 3).

We note that the computational cost added by the alignment term is negligible since it can be easily computed on GPU. This leads to a training time similar to the vanilla case where no alignment is used. The only required pre-processing is facial landmarks extraction which can be done off-line once and stored on disk. Action units map \mathbf{A} can be computed in a negligible time on CPU on the fly during training.

4 Results and Discussion

4.1 Experimental Methodology

Datasets. To evaluate our method, experiments are conducted on two standard datasets for the FER task: RAF-DB [39], and *AffectNet* [53].

- *RAF-DB* Real-world Affective Faces Database is a large scale facial expression dataset [39]. All images have been manually annotated by multiple annotators. It contains six basic expressions ('Happiness', 'Sadness', 'Surprise', 'Anger', 'Disgust', 'Fear') and 'Neutral'. The dataset contains 12,271 samples for training and 3,068 samples for testing. Both sets have the same distribution.

- *AffectNet* is one of the largest facial expression recognition datasets with 420k images were manually annotated. Following [37], 283,901 images are used for training, and 3,500 images for testing. In terms of labels, this dataset has the same six basic expressions as in the RAF-DB dataset, in addition to 'Neutral'.

Implementation Details. For all our experiments, we trained each method for 100 epochs over RAF-DB with a mini-batch size of 32 and 20 epochs for *AffectNet*, with a mini-batch size of 224. For CNN-based methods, we used ResNet50 [31] as an encoder. For transformer-based methods, we used DeiT-S [70] for TS-CAM [29]. For the APVIT method [82], we used their proposed transformer architecture which also relies on DeiT-S [70]. Images are aligned and resized to 256×256 , and randomly cropped patches of size 224×224 are extracted for training. For APVIT [82], images are resized to 112×112 and fed as input following the method's protocol. The hyper-parameter $\lambda > 0$ is estimated using validation by covering values that range from less than 1 to 20. The optimization of training loss is performed using stochastic gradient descent (SGD). The hyper-parameters search of different methods is done over the RAF-DB dataset. Due to its large size,

Methods / Case	RAF-DB				AffectNet			
	CL		CAM-COS		CL		CAM-COS	
	w/o AUs	w/ AUs	w/o AUs	w/ AUs	w/o AUs	w/ AUs	w/o AUs	w/ AUs
CNN-based								
CAM [93] (cvpr,2016)	88.20	88.95	0.55	0.70	60.88	62.37	0.56	0.69
WILDCAT [20] (cvpr,2017)	88.26	88.85	0.52	0.69	59.88	61.62	0.62	0.80
GradCAM [66] (iccv,2017)	88.39	88.85	0.55	0.74	60.77	62.08	0.53	0.75
GradCAM++ [10] (wacv,2018)	87.84	89.14	0.60	0.82	60.22	62.45	0.66	0.83
ACoL [89] (cvpr,2018)	87.94	88.68	0.54	0.67	58.28	61.48	0.55	0.65
PRM [95] (cvpr,2018)	88.13	88.88	0.48	0.59	57.77	60.97	0.52	0.75
ADL [13] (cvpr,2019)	87.45	88.65	0.50	0.63	57.88	61.25	0.54	0.66
CutMix [85] (eccv,2019)	88.39	88.59	0.55	0.57	58.74	59.88	0.56	0.58
LayerCAM [34] (ieee,2021)	87.90	88.88	0.60	0.84	60.77	62.45	0.66	0.83
Transformer-based								
TS-CAM [29] (iccv,2021)	86.70	88.00	0.58	0.71	58.99	59.54	0.57	0.58
APViT [82] (ieee,2022)	91.00	91.03	--	--	60.62	62.28	--	--

Table 1: **Classification (CL) and CAM-localization (CAM-COS)** performance over RAF-DB and AffectNet test sets with and without action units (AUs) across different methods.

Methods / Case	RAF-DB		AffectNet	
	w/o AUs	w/ AUs	w/o AUs	w/ AUs
	CNN-based			
CAM [93] (cvpr,2016)	0.57	0.85	0.64	0.82
WILDCAT [20] (cvpr,2017)	0.47	0.85	0.61	0.81
GradCAM [66] (iccv,2017)	0.63	0.85	0.65	0.82
GradCAM++ [10] (wacv,2018)	0.52	0.87	0.65	0.82
ACoL [89] (cvpr,2018)	0.46	0.84	0.60	0.81
PRM [95] (cvpr,2018)	0.43	0.85	0.55	0.82
ADL [13] (cvpr,2019)	0.51	0.85	0.65	0.83
CutMix [85] (eccv,2019)	0.51	0.80	0.57	0.82
LayerCAM [34] (ieee,2021)	0.52	0.86	0.65	0.82
Transformer-based				
TS-CAM [29] (iccv,2021)	0.55	0.88	0.48	0.79
APViT [82] (ieee,2022)	0.38	0.85	0.45	0.84

Table 2: **Attention-localization (ATT-COS)** (at layer 5) performance over RAF-DB and AffectNet test sets with and without action units (AUs).

relevant hyper-parameters are transferred from RAF-DB to AffectNet dataset.

Baseline Methods. To assess the benefits of using action unit cues, we leverage WSOL classifiers. They allow the classification of an image using only the image class as a label. In addition, they provide interpretability maps. In particular, we use CAM-based WSOL methods, which provide interpretability by highlighting ROIs associated with a class. To this end, we selected methods that cover both families of CAM techniques [62]: 1- Bottom-up methods where information flows from the input layer to the output layer. This

includes CAM [93], WILDCAT [20], ACoL [89], PRM [95], ADL [13], and TS-CAM [29]. 2- Top-down methods where information flows in both directions. This includes gradient-based methods: GradCAM [66], GradCAM++ [10], and LayerCAM [34]. All these methods are common in the WSOL field. In the FER task, we selected a recent state-of-the-art method, APViT [82], which builds spatial attention in its architecture to yield interpretable maps. However, it does not have a CAM module. All the methods are trained with and without our AUs loss in addition to classification loss in order to assess the impact of using action units as spatial cues for learning. We note that all results are reported using our own implementations.

To build action units map cues, we first extract standard 68 facial landmarks from images using SynergyNet [76]. Following [51], each facial expression can be recognized using only a set of generic action units. Using the extracted facial landmarks, one can build a 2D map that contains a heatmap of a single action unit. For an image, a single 2D heatmap is then built containing all the action units associated with the image expression. This heatmap encodes the location of the necessary discriminative spatial ROIs needed to recognize the facial expression presented in the image. Training a classifier to focus mainly only on these spatial ROIs in an image is expected to improve its interpretability and, furthermore, its classification accuracy. Note that the only manual supervision required for our method is the image expression. No extra manual annotations are required.

Evaluation Metrics. We use standard classification accuracy (CL) for the classification task. We also report a classification confusion matrix. Localization of action units is performed at CAM, and layer-wise attention maps. Although they are

both normalized between $[0, 1]$, they do not necessarily have the same exact value at the pixel level, compared to action units map, since attention is trained to be *correlated* with action unit maps. Therefore, we resort to using cosine similarity (Eq. 2)² as a localization (interpretability) measure to assess how a CAM or attention is well aligned with the action unit map. Higher similarity indicates better localization and, hence, better interpretability. We refer to the cosine similarity between a CAM and an action units map as $CAM-COS$ and as $ATT-COS$ for the case of attention map versus action units map. Similarly to the classification confusion matrix, we report a per-class cosine similarity matrix. We note that during training, we perform the model selection by taking the model with the best classification accuracy (CL), and we report its corresponding localization metrics.

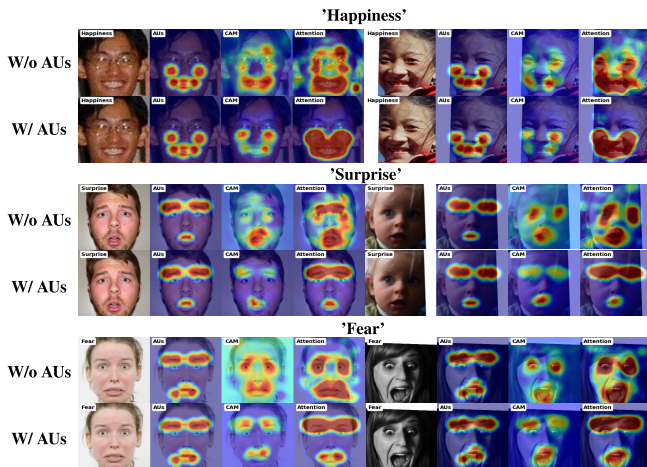


Figure 4: Illustration of interpretability prediction over RAF-DB test samples using CAM method [93] with and without action units alignment. From left to right: Input image, true action units map A , CAM $M[k]$, attention T_5 .

4.2 Comparison with different methods

Tab.1 shows the impact of using AUs alignment over classification and CAM interpretability across different methods. Overall, using our proposed action units alignment helped improving the CAM interpretability with large margin. Since CAMs are often built after the last layer where we applied the alignment, they are strongly affected leading to better AUs localization. We note that classification accuracy (CL) has also improved with relatively large margin over *AffectNet* compared to RAF-DB. This may be related to the fact there is still a large room for improvement in *AffectNet* compared to RAF-DB. In term of attention interpretability (Tab.2), the effect of using AUs loss is quite larger than in CAM. Most

²For evaluating a map, either a CAM or an attention map, it is first upsampled to the same size as the action units map A .

importantly, since the alignment is applied over layer-wise attention, it led to an attention that is better in interpretability than CAM. We note that achieving better classification accuracy does not necessarily mean better interpretability. For instance, vanilla APVIT method [82] has the highest classification accuracy CL of 91% over RAF-DB. However, it only scores 0.38 in term of attention interpretability $ATT-COS$, the lowest score across all models. Since vanilla case is optimized only to maximize classification score, it can easily find features, that are not necessarily interpretable, to achieve that. Interestingly, we show that the same model can achieve similar classification accuracy of 91.03% and an attention interpretability score of 0.85 when using our alignment loss. This suggests that spatial features have largely shifted their focus, as illustrated in Fig. 6, without compromising classification performance. As a result, the model finds different spatial features that satisfies both losses: classification and interpretability (AUs). We provide in Fig.4 an illustration of prediction with and without our action units alignment. In addition, Figs. 6, 7, 8, 9 show per-class average attention and CAM over both dataset. These visuals show better improvement of our classifier interpretability compared to vanilla case. We further more report per-class classification accuracy and localization over both dataset in Fig.10, 11. Overall, and across both dataset, we observe that the class 'Disgust' is the most difficult to localize its spatial cues.

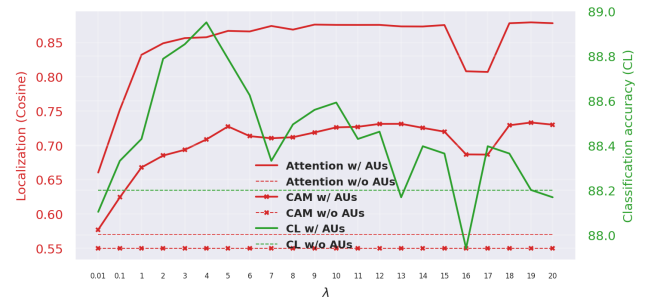


Figure 5: Ablations on the RAF-DB test set: impact of λ over classification and localization (interpretability) performance. Alignment to AUs is performed over layer 5 of ResNet50 [31] with CAM [93] method.

4.3 Ablation Studies

We performed two relevant ablations, assessing how classification and localization (interpretability) performance is affected by λ and at which layer the alignment loss is applied.

1- *Impact of λ* (Fig. 5). Given different values of λ , we report in Fig. 5 its impact on localization (red, left curves) on CAM, and attention at layer 5 using CAM method [93] and a ResNet50 backbone [31] over the RAF-DB dataset. It is observed that increasing λ improves localization at both CAM

Methods	CL	CAM-COS
CAM [93] w/o AUs	88.20	0.55
CAM [93] w/ AUs at layers:		
1	88.52	0.58
2	88.26	0.57
3	88.39	0.56
4	88.62	0.61
5	88.95	0.70
5+4	88.78	0.67
5+4+3	88.78	0.67
5+4+3+2	88.55	0.67
5+4+3+2+1	88.46	0.67

Table 3: Ablation study over RAF-DB test set: impact of applying AUs alignment over different layers over classification (CL) and CAM-localization (CAM-COS). Method: CAM [93] and ResNet50 [31] encoder. Layer 1 is the input layer.

and attention. However, localization performance starts to stagnate after $\lambda \approx 8$. Additionally, since the alignment with action units is performed at the attention level, localization at layer-wise attention (ATT-COS) is higher than at CAM-level (CAM-COS). However, they are still both better than their corresponding vanilla cases (dashed lines). In practice, although CAMs can be used for interpretability, the attention layer is shown to be more accurate and, hence, more reliable. We also report the impact of λ on classification accuracy (green, right curve). Increasing λ showed to improve localization since much importance is considered for the alignment loss term. Classification accuracy also kept improving until $\lambda \approx 4$. However, large values of λ put strong importance on localization compared to classification leading to degradation in classification accuracy. Hence, a compromise value is the one that improves localization without decreasing classification accuracy (e.g., $\lambda \approx 4$). Note that even large λ values can still yield relatively better classification accuracy compared to the vanilla case (dashed green line).

2- *At which layer should the alignment loss be applied?* (Table 3). Overall, applying our action units loss term across single or multiple layers improved both classification and CAM-localization. However, its application on the last feature layer has shown to be most beneficial. Top layers often capture semantic and most discriminative regions [86]. Since action unit maps highlight discriminative ROIs, using them to build better features at top layers is a reasonable choice. In all our experiments, we use the top layer for alignment.

5 Conclusion

In this work, we have introduced an approach to make FER models more interpretable. We extended the FER model training with an additional loss that favors feature maps whose average activations are similar to facial action unit activations. As in most datasets action units localizations are not available,

we estimate them by leveraging off-the-shelf facial point localizers and expert knowledge that associates action units to the corresponding emotion. By doing that, we manage to obtain a much more reliable and interpretable activation of the FER model that, in many cases, leads also to better recognition performance.

Acknowledgment

This research was supported in part by the Canadian Institutes of Health Research, the Natural Sciences and Engineering Research Council of Canada, and the Digital Research Alliance of Canada (alliancecan.ca).

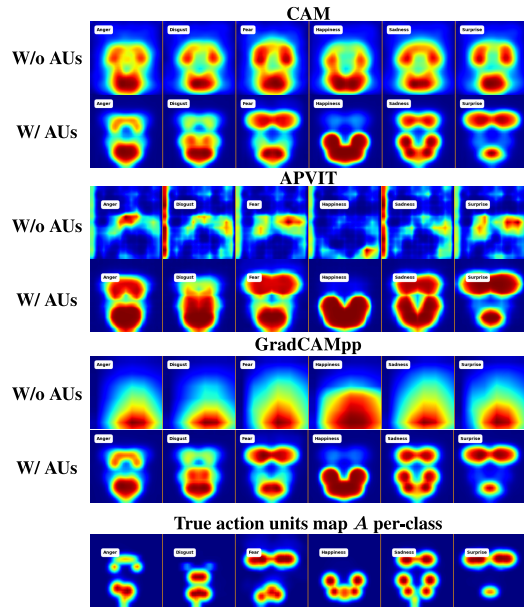


Figure 6: Illustration of **per-class average attention** maps over all test set of RAF-DB with and without action units alignment. Expressions from left to right: 'Anger', 'Disgust', 'Fear', 'Happiness', 'Sadness', 'Surprise'.

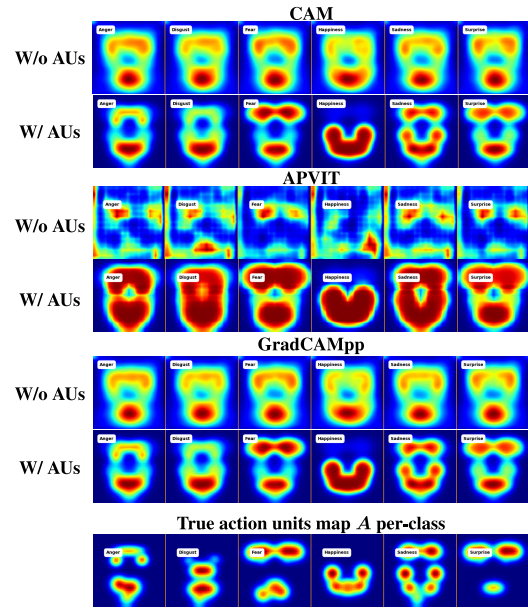


Figure 8: Illustration of **per-class average attention** maps over all test set of AffectNet with and without action units alignment. Expressions from left to right: 'Anger', 'Disgust', 'Fear', 'Happiness', 'Sadness', 'Surprise'.

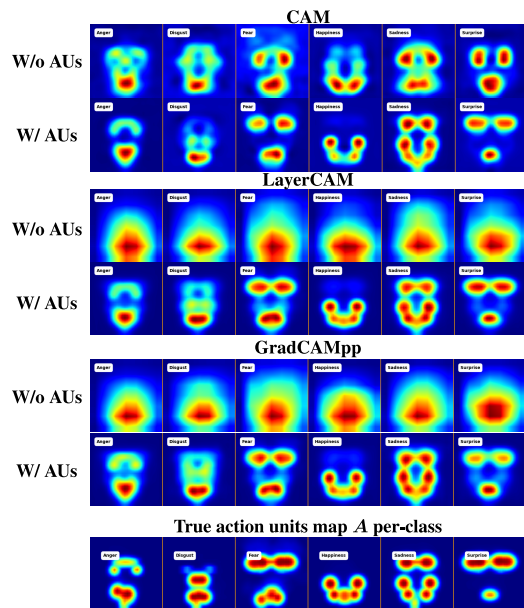


Figure 7: Illustration of **per-class average CAM** over all test set of RAF-DB with and without action units alignment. Expressions from left to right: 'Anger', 'Disgust', 'Fear', 'Happiness', 'Sadness', 'Surprise'.

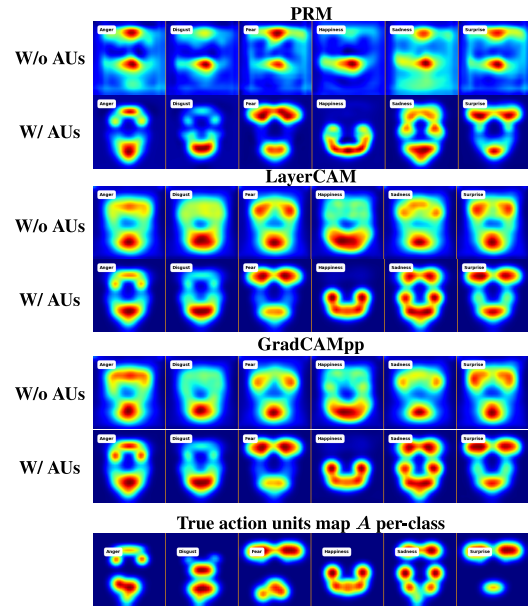


Figure 9: Illustration of **per-class average CAM** over all test set of AffectNet with and without action units alignment. Expressions from left to right: 'Anger', 'Disgust', 'Fear', 'Happiness', 'Sadness', 'Surprise'.

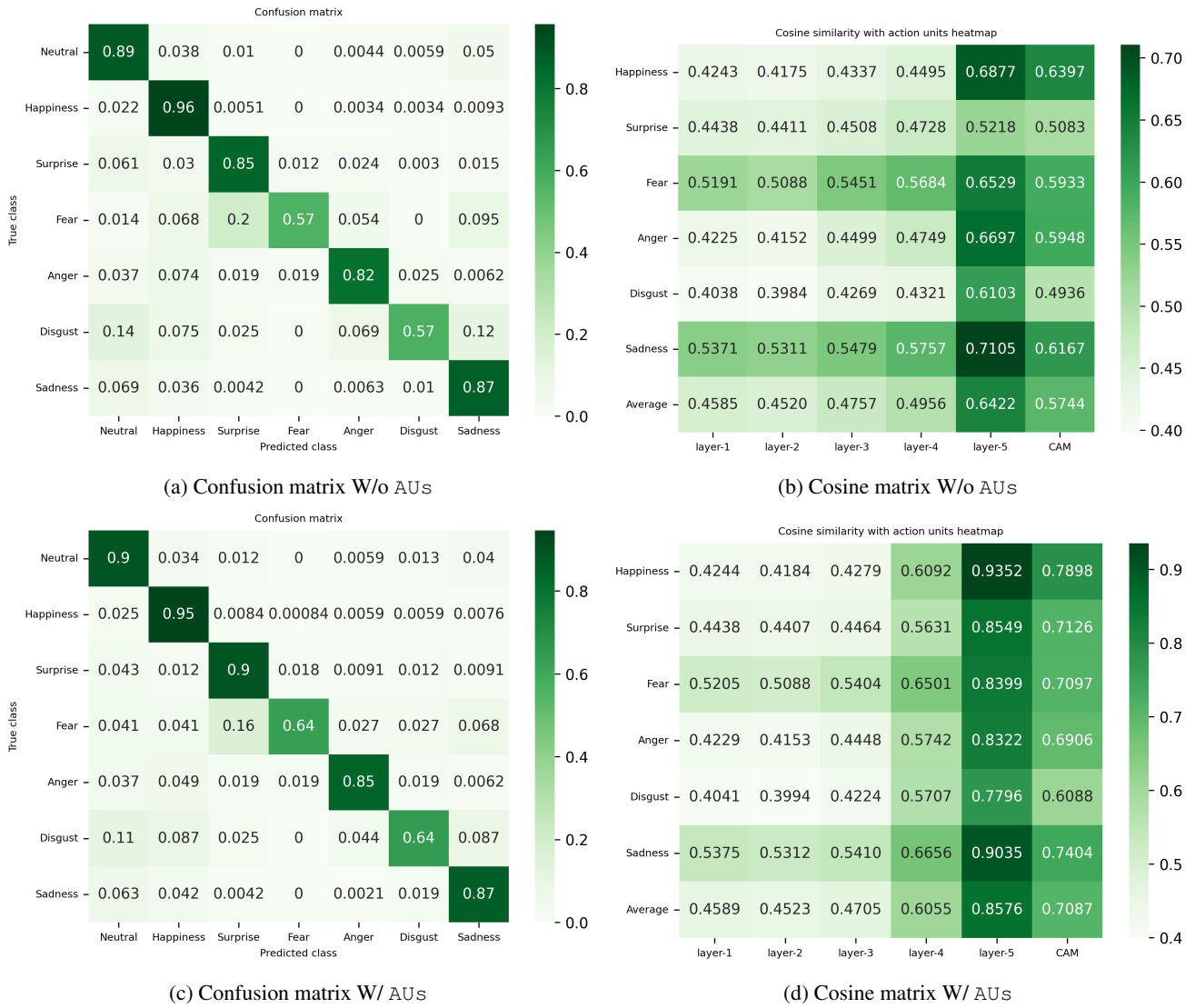


Figure 10: Confusion matrix and cosine matrix over RAF-DB test set with CAM method [93] with (top row) and without (bottom row) action units alignment. It show per-class and per-layer/CAM performance.

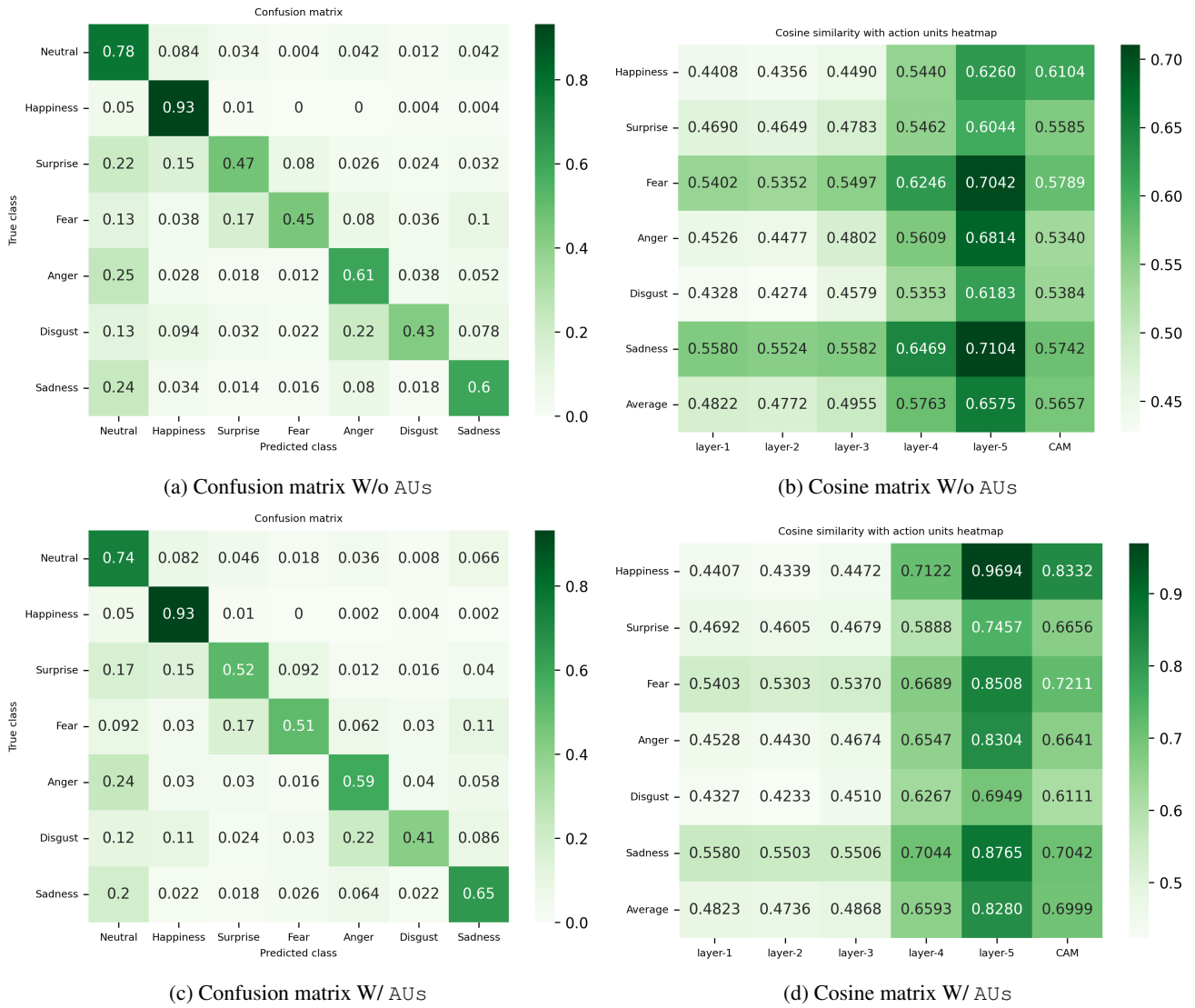


Figure 11: Confusion matrix and cosine matrix over AffectNet test set with CAM method [93] with (top row) and without (bottom row) action units alignment. It show per-class and per-layer/CAM performance.

References

- [1] T. Altameem and A. Altameem. Facial expression recognition using human machine interaction and multi-modal visualization analysis for healthcare applications. *Image and Vision Computing*, 103:104044, 2020.
- [2] M. A. Assari and M. Rahmati. Driver drowsiness detection using face expression recognition. In *ICSIPA*, 2011.
- [3] S. Belharbi, I. Ben Ayed, L. McCaffrey, and E. Granger. Tcam: Temporal class activation maps for object localization in weakly-labeled unconstrained videos. In *WACV*, 2023.
- [4] S. Belharbi, S. Murtaza, M. Pedersoli, I. Ben Ayed, L. McCaffrey, and E. Granger. Colo-cam: Class activation mapping for object co-localization in weakly-labeled unconstrained videos. *CoRR*, abs/2303.09044.
- [5] S. Belharbi, M. Pedersoli, I. Ben Ayed, L. McCaffrey, and E. Granger. Negative evidence matters in interpretable histology image classification. In *MIDL*, 2022.
- [6] S. Belharbi, J. Rony, J. Dolz, I. Ben Ayed, L. McCaffrey, and E. Granger. Deep interpretable classification and weakly-supervised segmentation of histology images via max-min uncertainty. *IEEE Transactions on Medical Imaging*, 41:702–714, 2022.
- [7] S. Belharbi, A. Sarraf, M. Pedersoli, I. Ben Ayed, L. McCaffrey, and E. Granger. F-cam: Full resolution class activation maps via guided parametric upscaling. In *WACV*, 2022.
- [8] J. Bonnard, A. Dapogny, F. Dhombres, and K. Bailly. Privileged attribution constrained deep networks for facial expression recognition. In *ICPR*, 2022.
- [9] C. Cao, X. Liu, Y. Yang, et al. Look and think twice: Capturing top-down visual attention with feedback convolutional neural networks. In *ICCV*, 2015.
- [10] A. Chattopadhyay, A. Sarkar, P. Howlader, and V. N. Balasubramanian. Grad-cam++: Generalized gradient-based visual explanations for deep convolutional networks. In *WACV*, 2018.
- [11] L.-Y. Chen, T.-H. Tsai, A. Ho, C.-H. Li, L.-J. Ke, L.-N. Peng, M.-H. Lin, F.-Y. Hsiao, and L.-K. Chen. Predicting neuropsychiatric symptoms of persons with dementia in a day care center using a facial expression recognition system. *Aging (Albany NY)*, 14(3):1280, 2022.
- [12] J. Choe, S. J. Oh, S. Lee, S. Chun, Z. Akata, and H. Shim. Evaluating weakly supervised object localization methods right. In *CVPR*, 2020.
- [13] J. Choe and H. Shim. Attention-based dropout layer for weakly supervised object localization. In *CVPR*, 2019.
- [14] P. Dabkowski and Y. Gal. Real time image saliency for black box classifiers. *NeurIPS*, 30, 2017.
- [15] N. Dalal and B. Triggs. Histograms of oriented gradients for human detection. In *CVPR*, 2005.
- [16] C. Darwing and P. Prodger. *The expression of the emotions in man and animals*. Oxford University Press, USA, 1998.
- [17] M. M. Deramgozin, S. Jovanovic, M. Arevalillo-HerrÁez, and H. Rabah. An explainable and reliable facial expression recognition system for remote health monitoring. In *ICECS*, 2022.
- [18] S. Desai and H. Ramaswamy. Ablation-cam: Visual explanations for deep convolutional network via gradient-free localization. In *WACV*, 2020.
- [19] F. Doshi-Velez and B. Kim. Towards a rigorous science of interpretable machine learning. *CoRR*, abs/1702.08608, 2017.
- [20] T. Durand, T. Mordan, N. Thome, and M. Cord. Wildcat: Weakly supervised learning of deep convnets for image classification, pointwise localization and segmentation. In *CVPR*, 2017.
- [21] T. Durand, N. Thome, and M. Cord. Weldon: Weakly supervised learning of deep convolutional neural networks. In *CVPR*, 2016.
- [22] P. Ekman and W. V. Friesen. Facial action coding system. *Environmental Psychology & Nonverbal Behavior*, 1978.
- [23] Y. Fan, J. Lam, and V. Li. Facial action unit intensity estimation via semantic correspondence learning with dynamic graph convolution. In *AAAI*, 2020.
- [24] A. H. Farzaneh and X. Qi. Facial expression recognition in the wild via deep attentive center loss. In *WACV*, 2021.
- [25] R. Fong, M. Patrick, and A. Vedaldi. Understanding deep networks via extremal perturbations and smooth masks. In *ICCV*, 2019.
- [26] R. C. Fong and A. Vedaldi. Interpretable explanations of black boxes by meaningful perturbation. In *ICCV*, 2017.
- [27] E. Friesen and P. Ekman. Facial action coding system: a technique for the measurement of facial movement. *Palo Alto*, 3(2):5, 1978.
- [28] R. Fu, Q. Hu, X. Dong, Y. Guo, Y. Gao, and B. Li. Axiom-based grad-cam: Towards accurate visualization and explanation of cnns. In *BMVC*, 2020.
- [29] W. Gao, F. Wan, X. Pan, Z. Peng, Q. Tian, Z. Han, B. Zhou, and Q. Ye. TS-CAM: token semantic coupled attention map for weakly supervised object localization. In *ICCV*, 2021.
- [30] S. Happy and A. Routray. Automatic facial expression recognition using features of salient facial patches. *IEEE Transactions on Affective Computing*, 6(1):1–12, 2014.
- [31] K. He, X. Zhang, S. Ren, and J. Sun. Deep residual learning for image recognition. In *CVPR*, 2016.
- [32] G. M. Jacob and B. Stenger. Facial action unit detection with transformers. In *CVPR*, 2021.
- [33] M. Jeong and B. C. Ko. Driver’s facial expression recognition in real-time for safe driving. *Sensors*, 18(12):4270, 2018.
- [34] P. Jiang, C. Zhang, Q. Hou, M. Cheng, and Y. Wei. Layercam: Exploring hierarchical class activation maps for localization. *IEEE Trans. Image Process.*, 30:5875–5888, 2021.
- [35] K. H. Kim, K. Park, H. Kim, B. Jo, S. H. Ahn, C. Kim, M. Kim, T. H. Kim, S. B. Lee, D. Shin, et al. Facial expression monitoring system for predicting patient’s sudden movement during radiotherapy using deep learning. *Journal of applied clinical medical physics*, 21(8):191–199, 2020.
- [36] J. Lee, E. Kim, S. Lee, J. Lee, and S. Yoon. Ficklenet: Weakly and semi-supervised semantic image segmentation using stochastic inference. In *CVPR*, 2019.
- [37] H. Li, N. Wang, X. Ding, X. Yang, and X. Gao. Adaptively learning facial expression representation via C-F labels and distillation. *IEEE Trans. Image Process.*, 30:2016–2028, 2021.
- [38] S. Li and W. Deng. Deep facial expression recognition: A survey. *IEEE transactions on affective computing*, 13(3):1195–1215, 2020.
- [39] S. Li, W. Deng, and J. Du. Reliable crowdsourcing and deep locality-preserving learning for expression recognition in the wild. In *CVPR*, 2017.
- [40] Y. Li, J. Zeng, S. Shan, and X. Chen. Occlusion aware facial expression recognition using cnn with attention mechanism. *IEEE Transactions on Image Processing*, 28(5):2439–2450, 2018.
- [41] Z. Li, T. Zhang, X. Jing, and Y. Wang. Facial expression-based analysis on emotion correlations, hotspots, and potential occurrence of urban crimes. *Alexandria Engineering Journal*, 60(1):1411–1420, 2021.
- [42] C. Liu, X. Zhang, X. Liu, T. Zhang, L. Meng, Y. Liu, Y. Deng, and W. Jiang. Facial expression recognition based on multi-modal features for videos in the wild. In *CVPR*, 2023.

- [43] D. Liu, H. Zhang, and P. Zhou. Video-based facial expression recognition using graph convolutional networks. In *ICPR*, 2021.
- [44] X. Liu, L. Jin, X. Han, J. Lu, J. You, and L. Kong. Identity-aware facial expression recognition in compressed video. In *ICPR*, 2021.
- [45] Y. Liu, W. Wang, C. Feng, H. Zhang, Z. Chen, and Y. Zhan. Expression snippet transformer for robust video-based facial expression recognition. *Pattern Recognition*, 138:109368, 2023.
- [46] Z. Liu, Y. Peng, and W. Hu. Driver fatigue detection based on deeply-learned facial expression representation. *Journal of Visual Communication and Image Representation*, 71:102723, 2020.
- [47] D. G. Lowe. Distinctive image features from scale-invariant keypoints. *Int. J. Comput. Vis.*, 60(2):91–110, 2004.
- [48] C. Luo, S. Song, W. Xie, L. Shen, and H. Gunes. Learning multi-dimensional edge feature-based AU relation graph for facial action unit recognition. In *IJCAI*, 2022.
- [49] J. Mai, M. Yang, and W. Luo. Erasing integrated learning: A simple yet effective approach for weakly supervised object localization. In *CVPR*, 2020.
- [50] J. Mao, R. Xu, X. Yin, Y. Chang, B. Nie, and A. Huang. POSTER V2: A simpler and stronger facial expression recognition network. *CoRR*, abs/2301.12149, 2023.
- [51] B. Martínez, M. F. Valstar, B. Jiang, and M. Pantic. Automatic analysis of facial actions: A survey. *IEEE Trans. Affect. Comput.*, 10(3):325–347, 2019.
- [52] A. Meethal, M. Pedersoli, S. Belharbi, and E. Granger. Convolutional stn for weakly supervised object localization and beyond. In *ICPR*, 2020.
- [53] A. Mollahosseini, B. Hassani, and M. H. Mahoor. Affectnet: A database for facial expression, valence, and arousal computing in the wild. *IEEE Trans. Affect. Comput.*, 10(1):18–31, 2019.
- [54] S. Murtaza, S. Belharbi, M. Pedersoli, A. Sarraf, and E. Granger. Constrained sampling for class-agnostic weakly supervised object localization. In *Montreal AI symposium*, 2022.
- [55] S. Murtaza, S. Belharbi, M. Pedersoli, A. Sarraf, and E. Granger. Discriminative sampling of proposals in self-supervised transformers for weakly supervised object localization. *CoRR*, abs/2209.09209, 2022.
- [56] S. Murtaza, S. Belharbi, M. Pedersoli, A. Sarraf, and E. Granger. Dips: Discriminative pseudo-label sampling with self-supervised transformers for weakly supervised object localization. *Image and Vision Computing*, page 104838, 2023.
- [57] R. Naidu, A. Ghosh, Y. Maurya, S. R. N. K., and S. S. Kundu. IS-CAM: integrated score-cam for axiomatic-based explanations. *CoRR*, abs/2010.03023, 2020.
- [58] Y. Nan, J. Ju, Q. Hua, H. Zhang, and B. Wang. A-mobilenet: An approach of facial expression recognition. *Alexandria Engineering Journal*, 61(6):4435–4444, 2022.
- [59] M. Oquab, L. Bottou, I. Laptev, and J. Sivic. Is object localization for free?-weakly-supervised learning with convolutional neural networks. In *CVPR*, 2015.
- [60] V. Petsiuk, A. Das, and K. Saenko. RISE: randomized input sampling for explanation of black-box models. In *BMVC*, 2018.
- [61] M. Puente Durán, D. Moreno Blanco, J. Solana Sánchez, P. Sánchez González, and E. J. Gómez Aguilera. A facial expression recognition system for ehealth intervention platforms: A proof of concept. 2019.
- [62] J. Rony, S. Belharbi, J. Dolz, I. Ben Ayed, L. McCaffrey, and E. Granger. Deep weakly-supervised learning methods for classification and localization in histology images: A survey. *Machine Learning for Biomedical Imaging*, 2:96–150, 2023.
- [63] M. Sajjad, F. U. M. Ullah, M. Ullah, G. Christodoulou, F. Alaya Cheikh, M. Hijji, K. Muhammad, and J. J. Rodrigues. A comprehensive survey on deep facial expression recognition: challenges, applications, and future guidelines. *Alexandria Engineering Journal*, 68:817–840, 2023.
- [64] W. Samek, G. Montavon, A. Vedaldi, L. K. Hansen, and K. Müller, editors. *Explainable AI: Interpreting, Explaining and Visualizing Deep Learning*, volume 11700 of *Lecture Notes in Computer Science*. Springer, 2019.
- [65] E. Sánchez-Lozano, G. Tzimiropoulos, and M. F. Valstar. Joint action unit localisation and intensity estimation through heatmap regression. In *BMVC*, 2018.
- [66] R. R. Selvaraju, M. Cogswell, A. Das, R. Vedantam, D. Parikh, and D. Batra. Grad-cam: Visual explanations from deep networks via gradient-based localization. In *ICCV*, 2017.
- [67] C. Shan, S. Gong, and P. W. McOwan. Facial expression recognition based on local binary patterns: A comprehensive study. *Image Vis. Comput.*, 27(6):803–816, 2009.
- [68] S. ter Stal, G. Jongbloed, and M. Tabak. Embodied Conversational Agents in eHealth: How Facial and Textual Expressions of Positive and Neutral Emotions Influence Perceptions of Mutual Understanding. *Interacting with Computers*, 33(2):167–176, 07 2021.
- [69] G. Tonguç and B. O. Ozkara. Automatic recognition of student emotions from facial expressions during a lecture. *Computers & Education*, 148:103797, 2020.
- [70] H. Touvron, M. Cord, M. Douze, F. Massa, A. Sablayrolles, and H. Jégou. Training data-efficient image transformers & distillation through attention. In *ICML*, 2021.
- [71] M. F. Valstar, M. Mehu, B. Jiang, M. Pantic, and K. Scherer. Meta-analysis of the first facial expression recognition challenge. *IEEE Transactions on Systems, Man, and Cybernetics, Part B (Cybernetics)*, 42(4):966–979, 2012.
- [72] A. Vellido. The importance of interpretability and visualization in machine learning for applications in medicine and health care. *Neural computing and applications*, 32(24):18069–18083, 2020.
- [73] J. Wang, A. Bhalerao, T. Yin, S. See, and Y. He. Camanet: class activation map guided attention network for radiology report generation. *IEEE Journal of Biomedical and Health Informatics*, 2024.
- [74] K. Wang, X. Peng, J. Yang, D. Meng, and Y. Qiao. Region attention networks for pose and occlusion robust facial expression recognition. *IEEE Transactions on Image Processing*, 29:4057–4069, 2020.
- [75] J. Wei, Q. Wang, Z. Li, S. Wang, S. K. Zhou, and S. Cui. Shallow feature matters for weakly supervised object localization. In *CVPR*, 2021.
- [76] C.-Y. Wu, Q. Xu, and U. Neumann. Synergy between 3dmm and 3d landmarks for accurate 3d facial geometry. In *3DV*, 2021.
- [77] P. Wu, W. Zhai, Y. Cao, J. Luo, and Z. Zha. Spatial-aware token for weakly supervised object localization. In *ICCV*, 2023.
- [78] X. Xiao, Y. Shi, and J. Chen. Towards better evaluations of class activation mapping and interpretability of cnns. In *International Conference on Neural Information Processing*, pages 352–369, 2023.
- [79] S. Xie and H. Hu. Facial expression recognition using hierarchical features with deep comprehensive multipatches aggregation convolutional neural networks. *IEEE Transactions on Multimedia*, 21(1):211–220, 2018.
- [80] S. Xie, H. Hu, and Y. Wu. Deep multi-path convolutional neural network joint with salient region attention for facial expression recognition. *Pattern recognition*, 92:177–191, 2019.

- [81] F. Xue, Q. Wang, and G. Guo. Transfer: Learning relation-aware facial expression representations with transformers. In *ICCV*, 2021.
- [82] F. Xue, Q. Wang, Z. Tan, Z. Ma, and G. Guo. Vision transformer with attentive pooling for robust facial expression recognition. *IEEE Transactions on Affective Computing*, 2022.
- [83] K. Yadav. *Explaining human emotions using interpretable machine learning for behavioral and mental healthcare*. PhD thesis, 2022.
- [84] G. Yolcu, I. Oztel, S. Kazan, C. Oz, K. Palaniappan, T. E. Lever, and F. Bunyak. Deep learning-based facial expression recognition for monitoring neurological disorders. In *International Conference on Bioinformatics and Biomedicine (BIBM)*, 2017.
- [85] S. Yun, D. Han, S. Chun, S. Oh, Y. Yoo, and J. Choe. Cutmix: Regularization strategy to train strong classifiers with localizable features. In *ICCV*, 2019.
- [86] M. D. Zeiler and R. Fergus. Visualizing and understanding convolutional networks. In *ECCV*, 2014.
- [87] J. Zhang, S. A. Bargal, Z. Lin, et al. Top-down neural attention by excitation backprop. *International Journal of Computer Vision*, 126(10):1084–1102, 2018.
- [88] Q. Zhang, L. Rao, and Y. Yang. A novel visual interpretability for deep neural networks by optimizing activation maps with perturbation. In *AAAI*, 2021.
- [89] X. Zhang, Y. Wei, J. Feng, Y. Yang, and T. Huang. Adversarial complementary learning for weakly supervised object localization. In *CVPR*, 2018.
- [90] X. Zhang, Y. Wei, and Y. Yang. Inter-image communication for weakly supervised localization. In A. Vedaldi, H. Bischof, T. Brox, and J. Frahm, editors, *ECCV*, Lecture Notes in Computer Science, 2020.
- [91] Y. Zhang, R. Zhao, W. Dong, B.-G. Hu, and Q. Ji. Bilateral ordinal relevance multi-instance regression for facial action unit intensity estimation. In *CVPR*, 2018.
- [92] C. Zheng, M. Mendieta, and C. Chen. POSTER: A pyramid cross-fusion transformer network for facial expression recognition. In *ICCVw*, 2023.
- [93] B. Zhou, A. Khosla, A. Lapedriza, A. Oliva, and A. Torralba. Learning deep features for discriminative localization. In *CVPR*, 2016.
- [94] X. Zhou, K. Jin, Y. Shang, and G. Guo. Visually interpretable representation learning for depression recognition from facial images. *IEEE transactions on affective computing*, 11(3):542–552, 2018.
- [95] Y. Zhou, Y. Zhu, Q. Ye, Q. Qiu, and J. Jiao. Weakly supervised instance segmentation using class peak response. In *CVPR*, 2018.
- [96] Y. Zhu, Y. Zhou, Q. Ye, et al. Soft proposal networks for weakly supervised object localization. In *ICCV*, 2017.